

# PCA-Based Out-of-Sample Extension for Dimensionality Reduction

Yariv Aizenbud      Amit Bermanis      Amir Averbuch

November 4, 2015

## Abstract

Dimensionality reduction methods are very common in the field of high dimensional data analysis. Typically, algorithms for dimensionality reduction are computationally expensive. Therefore, their applications for the analysis of massive amounts of data are impractical. For example, repeated computations due to accumulated data are computationally prohibitive. In this paper, an out-of-sample extension scheme, which is used as a complementary method for dimensionality reduction, is presented. We describe an algorithm which performs an out-of-sample extension to newly-arrived data points. Unlike other extension algorithms such as Nyström algorithm, the proposed algorithm uses the intrinsic geometry of the data and properties for dimensionality reduction map. We prove that the error of the proposed algorithm is bounded. Additionally to the out-of-sample extension, the algorithm provides a degree of the abnormality of any newly-arrived data point.

## 1 Introduction

Analysis of large amounts of high-dimensional big data is of great interest since it illuminates the underlying phenomena. To cope with high-dimensional big data, it is sometimes assumed that there are some (unobservable) dependencies between the parameters of the multidimensional data points. Mathematically, it means that the data is sampled from a low-dimensional manifold that is embedded in a high dimensional ambient space. Dimensionality reduction methods, which rely on the presence of a manifold, map the data

into a low-dimensional space while preserving certain qualities of the low-dimensional structures of the data.

A broad class of dimensionality reduction methods are based on kernel-based methods. The kernel encapsulates a measure of mutual affinities (or similarities) between data points. Particularly, if the kernel is semi-positive definite, it can be considered as Gram matrix of inner products, which correspond to an implicit mapping of the data to a high dimensional space, typically referred to as the feature space. Depending on the chosen kernel, the new geometry of the data in feature space, represents important features of the data.

Kernel-PCA is a technique that generalizes the well known principal component analysis (PCA) [12, 13]. While the latter detects principal directions of data in Euclidean space and then projects the data onto them, the former does the same in the feature space. It is resulted in a low dimensional Euclidean representation (embedding) of the data that approximates the feature space geometry. The dimensionality of the embedding space is affected by the decay rate of the kernel's spectrum. Examples of kernel methods are diffusion maps (DM) [6], local linear embedding (LLE) [20], Laplacian eigenmaps [2], Hessian eigenmaps [10] and local tangent space alignment [23, 24].

From a practical point of view, kernel methods have a significant computational drawback: spectral analysis of the kernel matrix becomes impractical for large datasets due to high computational complexity required to manipulate a kernel matrix. Their global nature is also disadvantageous. Furthermore, in many applications, the analysis process is dynamic due to data accumulation over time and, as a result, the embedding has to be modified once in a while. Processing a kernel matrix in memory becomes impractical for large datasets due to their sizes.

A general solution scheme embeds a subset of the source data that is usually referred to as a training dataset. Then, the embedding is extended to any out-of-sample data point. The Nyström method [1, 9, 17], which is widely used in integral equations solvers, has become very popular as an out-of-sample extension method associated with dimensionality reduction methodology. For a review of spectral clustering and Nyström extension see Section 2 in [21]. The Nyström extension scheme has three significant disadvantages: (a) It requires diagonalization of a matrix that costs  $O(n^3)$  operations [11]. (b) It requires working with a matrix which may be ill-conditioned due to fast decay of its spectrum, and (c) it is unclear how to choose the length parameter  $\epsilon$  since the output

is sensitive to the choice of  $\epsilon$ . Some limitations of Nyström extension are overcome in [4]. Geometric Harmonics (GH) [7] is another out-of-sample extension method. It uses the Nyström extension of eigenfunctions of a kernel defined on the data. In order to avoid numerical instabilities, it uses only the significant spectral components. In that sense, the GH framework filters out high frequencies, which are determined by the kernel, rather than by the data. This problem, additionally to the fixed interpolation distance problem, is treated in [19], where a multiscale interpolation scheme is introduced. Another multiscale approach, which aims to solve the aforementioned limitations, was recently introduced in [4]. Both methods project the objective function on the eigencomponents of a series of kernels, which cover the complete spectrum of that function. The difference between these methods is in the extraction of principal components while the former is spectral and the latter is interpolative.

All these methods use a kernel matrix (or, perhaps, its low rank approximation) as an interpolation matrix. This mechanism is strongly related to a variety of isotropic interpolation methods that employ radial basis functions (RBF). Such methods are used for scattered data approximation, where the data lies in a metric space. More details about RBF and scattered data approximation can be found in [5] and [22], respectively.

In this paper, we employ the manifold assumption to establish an anisotropic out-of-sample extension. We suggest a new anisotropic interpolation scheme that ascribes for each data point a likelihood neighborhood. This likelihood is based on geometric features from the dimensionality reduction map by using PCA of the map's image. Incorporation of such neighborhood information produces a linear system for finding the out-of-sample extension for this data point. This method also provides an abnormality measure for a newly-mapped data point.

The paper has the following structure: Section 2 introduces the problem and the needed definitions. The construction of the out-of-sample extension is described in section 3. Section 4 establishes the geometric-based stochastic linear system on which the interpolant is based. Three different interpolants are presented where each is based on different geometric considerations. In Section 5, an analysis of interpolation's error is presented for the case of Lipschitz mappings. Computational complexity analysis of the scheme is presented in Section 6. Experimental results for both synthetic data and real-life data are presented in Section 7.

## 2 Problem Setup

Let  $\mathcal{M}$  be a compact low-dimensional manifold of intrinsic dimension  $m$  that lies in a high-dimensional ambient space  $\mathbb{R}^n$  ( $m < n$ ), whose Euclidean metric is denoted by  $\|\cdot\|$ . Let  $\psi$  be a smooth, Lipschitz and dimensionality reducing function defined on  $\mathcal{M}$ , i.e.  $\psi : \mathcal{M} \rightarrow \mathcal{N} \subset \mathbb{R}^d$  ( $m < d < n$ ), where  $\mathcal{N}$  is a  $m$ -dimensional manifold. Let  $M = \{x_1, \dots, x_p\} \subset \mathcal{M}$  be a finite training dataset, sufficiently dense sampled from  $\mathcal{M}$ , whose image  $\psi(M) = \{\psi(x_1), \dots, \psi(x_p)\}$  under  $\psi$  was already computed. Given an out-of-sample data point  $x \in \mathcal{M} \setminus M$ , we aim to embed it into  $\mathbb{R}^d$  while preserving some local properties of  $\psi$ . The embedding of  $x$  into  $\mathbb{R}^d$  is denoted by  $\hat{\psi}(x)$ . It is referred to as the extension of  $\psi$  to  $x$ .

The proposed extension scheme is based on the local geometric properties of  $\psi$  in the neighborhood of  $x$ , denoted by  $N(x)$ . Specifically, the influence of a neighbor  $x_j \in N(x)$  on the value of  $\hat{\psi}(x)$  depends on its distance from  $x$  and the geometry of the image  $\psi(N(x))$  of  $N(x)$  under  $\psi$ . This approach is reflected by considering  $\hat{\psi}(x)$  as a random variable with mean  $\mathbb{E}\hat{\psi}(x) = \psi(x_j)$  and a variance  $\mathbb{V}\hat{\psi}(x)$  that depends on both the distance of  $x$  from  $x_j$  and on some geometric properties of  $\psi(N(x))$  that will be detailedly discussed in Section 4.2. Mathematically,

$$\hat{\psi}(x) = \psi(x_j) + \omega_j, \quad (2.1)$$

where  $\omega_j$  is a random variable with mean  $\mathbb{E}\omega_j = 0$  and variance  $\mathbb{V}\omega_j = \sigma_j$  that, as previously mentioned, depends on the local geometry of  $\psi$  in the neighborhood  $N(x)$  of  $x$ . Thus, we get  $|N(x)|$  equations for evaluating  $\hat{\psi}(x)$ , one for each neighbor  $x_j \in N(x)$ . The optimal solution then, is achieved by the generalized least squares approach described in Section 2.1.

### 2.1 Generalized Least Squares (GLS)

In this section, we briefly describe the GLS approach that will be utilized to evaluate  $\hat{\psi}(x)$ . In general, the GLS addresses the problem of a linear regression that assumes neither independence nor common variance between the random variables. Thus, if  $y = (y_1, \dots, y_k)^T$  are random variables that correspond to  $k$  data points in  $\mathbb{R}^d$ , the addressed regression problem is

$$y = X\beta + \mu, \quad (2.2)$$

where  $X$  is an  $k \times d$  matrix that stores the data points as its rows and  $\mu \in \mathbb{R}^k$  is an error vector. Respectively to the aforementioned assumption, the  $k \times k$  conditional covariance matrix of the error term  $W = \mathbb{V}\{\mu|X\}$  is not necessarily scalar or diagonal. The GLS solution to Eq. 2.2 is

$$\hat{\beta} = (X^T W^{-1} X)^{-1} X^T W^{-1} y. \quad (2.3)$$

The Mahalanobis distance between two random vectors  $v_1$  and  $v_2$  of the same distribution with conditional covariance matrix  $W$  is

$$\|v_1 - v_2\|_W \triangleq \sqrt{(v_1 - v_2)^T W^{-1} (v_1 - v_2)}. \quad (2.4)$$

**Observation 2.1.** *The Mahalanobis distance in Eq. 2.4 measures the similarity between  $v_1$  and  $v_2$  in respect to  $W$ . If the random variables are independent, then  $W$  is diagonal. Then, it is more affected by low variance random variables and less by high variance variables.*

The GLS solution from Eq. 2.3, minimizes the squared Mahalanobis distance between  $y$  and the estimator  $X\beta$ , i.e.

$$\hat{\beta} = \arg \min_{\beta \in \mathbb{R}^d} \|y - X\beta\|_W. \quad (2.5)$$

Further details concerning GLS can for example be found in [14].

In our case, for a fixed out-of-sample data point  $x \in \mathcal{M} \setminus M$  with its  $k = |N(x)|$  neighbors, a linear system of  $k$  equations, each of the form of Eq. 2.1, is solved for  $\hat{\psi}(x)$ . Without loss of generality, we assume that  $N(x) = \{x_1, \dots, x_k\}$ . The matrix formulation of such a system is

$$J\hat{\psi}(x) = \Psi + \Omega, \quad (2.6)$$

where  $J = [I_d, \dots, I_d]^T$  is the  $kd \times d$  identity blocks matrix,  $\Omega$  is a  $kd$ -long vector, whose  $j$ -th section is the  $d$ -long constant vector  $(\omega_j, \dots, \omega_j)^T$  and  $\Psi$  is a  $kd$ -long vector, whose  $j$ -th section is the  $d$ -long vector  $\psi(x_j)$ . The vector  $\Psi$  encapsulates the images of  $N(x)$  under  $\psi$  such as the neighborhood of  $\hat{\psi}(x)$  in  $\mathcal{N}$ . The corresponding covariance matrix is the  $kd \times kd$  blocks diagonal matrix  $W$ ,

$$W = \text{diag}(w_1, \dots, w_k), \quad (2.7)$$

whose  $j$ -th diagonal element is  $w_j = \sigma_j^2 I_d$ . Therefore, due to Eq. 2.3, the GLS solution to Eq. 2.6 is

$$\hat{\psi}(x) \triangleq (J^T W^{-1} J)^{-1} J^T W^{-1} \Psi, \quad (2.8)$$

and it minimizes the Mahalanobis distance

$$m(x) \triangleq \|J\hat{\psi}(x) - \Psi\|_W \quad (2.9)$$

that measures the similarity (with respect to  $W$ ) between  $\hat{\psi}(x)$  and its neighbors  $\{\psi(x_1), \dots, \psi(x_k)\}$  in  $\mathcal{N}$ , which are encapsulated in  $\Psi$ . Once  $W$  is defined as an invertible covariance matrix of  $\hat{\psi}(x)$ , as defined in Eq. 2.8, is well posed. The definition of  $W$  depends on the definition of  $w_j$  for any  $j = 1, \dots, k$ , which can be chosen subjected to the similarity properties to be preserved by  $\psi$ . These properties are discussed in Section 4. Once Eq. 2.8 is solved for  $\hat{\psi}(x)$ , the Mahalanobis distance from Eq. 2.9 provides a measure for the disagreement between the out-of-sample extension of  $\psi$  and  $x$  with the surrounding geometry. Thus, a large value of  $m(x)$  (Eq. 2.9) indicates that  $x$  resides outside of  $\mathcal{M}$  and thus, in data analysis terminology, it can be considered as an anomalous data point.

### 3 Construction of the out-of-sample extension

As mentioned in Section 2.1, the GLS solution minimizes the Mahalanobis distances between  $\hat{\psi}(x)$  and its neighbors according to the stored information in  $W$ . Thus, if the variances are determined subjected to some feature, then  $\hat{\psi}(x)$ , which is defined in Eq. 2.8, is the closest point in  $\mathcal{N}$  to its neighbors with respect to this feature.

The idea of Algorithm 3.1 is to get a linear approximation for the local geometry of  $\psi$  and then device an out-of-sample extension that best preserves that linear demand using GLS. The GLS solution also provides the error, which, as described in section 2.1,

is considered as an anomalous score.

---

**Algorithm 3.1:** PCA-Based Out-Of-Sample Extension

---

**Input:**  $M = \{x_1, \dots, x_n\} \in \mathbb{R}^m$  - training dataset.

$Y = \{y_1, \dots, y_n\} = \{\psi(x_1), \dots, \psi(x_n)\}$  - training dataset after dimensionality reduction.

$x$  - an out of sample data point.

**Output:**  $y$  - an out-of-sample extension of the data point  $x$  that preserves the local properties of  $\psi$ .

$err$  - an abnormality score of the data point  $x$ .

- 1: Find a set  $N_\varepsilon(x)$  (Eq. 4.1) of the nearest neighbors with radius  $\varepsilon$  to the data point  $x$  in  $M$ .
  - 2: For each data point  $x_i \in N_\varepsilon(x)$ , construct a weighted linear system  $W\psi(x_i) = y$  for  $y$  where the construction of  $W$  is described in section 4.
  - 3:  $y$  is the optimal solution for the combined weighted linear system, as described in section 2.1.
  - 4: When GLS is solved, find the residual  $err$  of the solution.
- 

## 4 Geometric-based covariance matrix

In this section we present a construction of  $W$ , which is the weight of the linear system for  $y$ , such that the resulted out-of-sample extension  $\hat{\psi}(x)$  agrees with principal direction of its neighborhood in  $\mathcal{N}$ . The neighborhood  $N_\varepsilon(x)$  can be defined variously. In this paper, we use the definition

$$N_\varepsilon(x) \triangleq \{y \in M : \|x - y\| \leq \varepsilon\}, \quad (4.1)$$

for some positive  $\varepsilon$ , which ensures locality of the extension scheme. The parameter  $\varepsilon$  should be fixed according to the sampling density of  $\mathcal{M}$  such that  $|N_\varepsilon(x)| \geq d$ . This restriction enables to detect the principal directions of the image of  $\psi(N_\varepsilon(x))$  in  $\mathcal{N}$ .

In the rest of this section, we present the construction of  $W$ . The first construction, presented in Section 4.1 provides a mechanism to control the rate of influence of a data point  $x_j \in N_\varepsilon(x)$  on the value of  $\hat{\psi}(x)$  as a function of its distance from  $x$ . The second construction for  $W$ , presented in Section 4.2, incorporates information regarding principal variance directions of  $N_\varepsilon(x)$  such that the resulted out-of-sample extension  $\hat{\psi}(x)$  “agrees”

with these directions.

## 4.1 Distance based covariance matrix $W$

Although the definition of  $N_\varepsilon(x)$  provides locality for the scheme computation, it is reasonable to require that data points in  $N_\varepsilon(x)$ , which are distant from  $x$ , affect less than close data points. For this purpose, an “affection weight”

$$\lambda_j \triangleq \frac{1}{\|x - x_j\|} \quad (4.2)$$

is assigned to each data point  $x_j \in N_\varepsilon(x)$ . Of course, any other decreasing function of the distance between  $x$  and  $x_j$  can be utilized. By defining the variance  $\sigma_j$  to be proportional to the distance  $\|x - x_j\|$  such that  $\sigma_j \triangleq \lambda_j^{-1}$ , then we get a diagonal matrix  $W$ , whose  $j$ -th diagonal element is

$$w_j \triangleq \lambda_j^2 I_d. \quad (4.3)$$

Thus, due to Observation 2.1, close data points in  $N_\varepsilon(x)$  affect  $\hat{\psi}(x)$  more than data points that are far away.

## 4.2 Tangential space based covariance matrix $W$

In this section, we present a covariance matrix that encapsulates geometric information concerning the manifold  $\mathcal{N}$ . The covariance matrix  $W$  is set such that the resulted extension obeys the Lipschitz property of  $\psi$ .

Let  $\mathcal{T}_j$  be the tangential space to  $\mathcal{N}$  in  $\psi(x_j)$  and let  $\mathcal{P}_j$  be the orthogonal projection on  $\mathcal{T}_j$ . We denote the tangential component of  $\omega_j$  by  $\omega_j^t = \mathcal{P}_j \omega_j$ , and its orthogonal complement by  $\omega_j^o = (\mathcal{I} - \mathcal{P}_j) \omega_j$ , where  $\mathcal{I}$  is the identity transformation. Proposition 4.1 quantifies the tangential and perpendicular components of  $\omega_j$  from Eq. 2.1, as functions of the curvature of  $\mathcal{N}$  in  $x_j$  and  $\|x - x_j\|$ .

**Proposition 4.1.** *Let  $\|x - x_j\| \leq r$  and assume that the curvature of  $\mathcal{N}$  in  $x_j$  is bounded by a constant  $c_j$ . If  $\psi$  is a Lipschitz function with constant  $k$ , then  $\omega_j^t \leq kr$  and  $\omega_j^o \leq (c_j k r)^2$ .*

*Proof.* Without loss of generality it is assumed that  $\psi(x_j) = 0 \in \mathbb{R}^d$  and  $\mathcal{T}_j = \mathbb{R}^m$ . We denote the graph of the manifold  $\mathcal{N}$  in the neighborhood of 0 by the function  $f : \mathcal{T}_j \rightarrow \mathbb{R}^{d-m}$ , where the data points in  $\mathcal{N}$  are  $(z, f(z))$ ,  $z \in \mathcal{T}_j$ . Thus we get  $f(0) = 0$  and  $\frac{\partial f}{\partial z}(0) =$



0. Let  $x \in \mathcal{M}$  be a data point in the neighborhood of  $x_j$  and let  $\psi(x) = (z_x, f(z_x))$ . Namely,  $z_x = \mathcal{P}_j\psi(x)$  and  $f(z_x) = (\mathcal{I} - \mathcal{P}_j)\psi(x)$ . Then, the Taylor expansion of  $f(z_x)$  around 0 yields  $f(z_x) = f(0) + \frac{\partial f}{\partial z}(0)(z_x) + O(\|z_x\|^2)$ . Since  $\psi$  is assumed to be a Lipschitz function with constant  $k$ , we get  $\|z_x\| = \|\mathcal{P}_j(\psi(x) - \psi(x_j))\| \leq \|\psi(x) - \psi(x_j)\| \leq kr$ . Thus, we get that  $\|\omega_j^t\| = \|\mathcal{P}_j(\psi(x) - \psi(x_j))\| \leq kr$  and  $\|\omega_j^o\| \leq (c_jkr)^2$ .  $\square$

From Eq. 2.1, Proposition 4.1 provides a relation between the tangential and perpendicular components of  $\omega_j$ . Thus,  $\Omega$  from Eq. 2.6 is the  $kd$ -long vector, whose  $j$ -th section is the  $d$ -long vector  $(\omega_j^t, \dots, \omega_j^t, \omega_j^o, \dots, \omega_j^o)^T$ , where its first  $m$  entries are the tangential weights and the rest  $d - m$  are the perpendicular weights. The corresponding covariance matrix is the  $kd \times kd$  blocks diagonal matrix  $W$ , whose  $j$ -th diagonal element is the  $d \times d$  diagonal matrix

$$w_j = \begin{pmatrix} \lambda_j^2 & & & & & & & & \\ & \ddots & & & & & & & \\ & & \lambda_j^2 & & & & & & \\ & & & (c\lambda_j)^4 & & & & & \\ & & & & \ddots & & & & \\ & & & & & & & & (c\lambda_j)^4 \end{pmatrix},$$

where the first  $m$  diagonal elements are  $\lambda_j^2$  (see Eq. 4.2), and the rest  $d - m$  are  $(c\lambda_j)^4$ . Then, the solution is given by Eq. 2.6 while  $J$  and  $\Psi$  remain the same.

#### 4.2.1 Tangential Space Approximation

In real life applications, in order to use the tangential space to  $\mathcal{N}$  in  $\psi(x_j)$ , it has to be first approximated by using its neighboring data. In this section, we approximate the tangential space and the principle directions of the manifold  $\mathcal{N}$  at  $\psi(x_j)$ . Then, these approximations are incorporated in the construction of  $W$  to ascribe heavy weights to the tangential direction and less significant weights to the perpendicular ones. The principle directions of the data and the variance of each direction are the eigenvectors and eigenvalues of the covariance matrix of a data points  $\psi(x_j)$ , respectively. This covariance matrix is also known as the PCA matrix. A multi-scale version of the local PCA algorithm is analyzed in [15] and it can be used in our analysis. It is important to take at least as many data points as the dimensionality of  $\mathcal{N}$ .

The covariance matrix of a data point  $\psi(x_j)$  is computed in the following way: for

simplicity of calculations, we take as the set of neighbors of  $\psi(x_j)$  the set  $\psi(N_{\varepsilon_1}(x)) = \psi(x_1), \dots, \psi(x_k)$ . Then, we form the  $k \times d$  matrix  $X$ , whose rows in the aforementioned set are

$$X = \begin{pmatrix} -\psi(x_1) - \\ \vdots \\ -\psi(x_k) - \end{pmatrix}.$$

Accordingly, we define

$$\text{cov}(\psi(x_j)) \triangleq \left(\frac{1}{\varepsilon_1^2}\right) \left(\frac{1}{k}\right) X X^t, \quad \text{for all } i = 1, \dots, k. \quad (4.4)$$

Since we take the same set of data points then for all  $i$  and  $j$  we have  $\text{cov}(\psi(x_j)) = \text{cov}(\psi(x_i))$ . To make the calculation and stability issues easier we add the  $(c \cdot \lambda_i)^4$  component to all the diagonal components. Consequently, we define:

$$w_j \triangleq \left( \lambda_j^{-2} \text{cov}(\psi(x_j)) + \begin{pmatrix} (c \cdot \lambda_j)^{-4} & 0 & \dots & 0 \\ 0 & (c \cdot \lambda_j)^{-4} & \dots & 0 \\ \vdots & \ddots & \ddots & \vdots \\ 0 & \dots & 0 & (c \cdot \lambda_j)^{-4} \end{pmatrix} \right)^{-1}. \quad (4.5)$$

Since  $w_i$  is positive definite, it is invertible. We notice that it was possible to add the  $(c \cdot \lambda_i)^{-4}$  weight components only to the least significant directions of the covariance matrix by computing the SVD [15] of the covariance matrix. This does not improve the accuracy significantly but adds more complexity to the computation.  $W$  is a block diagonal matrix with the same structure as appears in Eq. 2.7.

Another option is to make different estimations for the tangential space in different data points by using different sets of data points in the covariance matrix computation. While this estimation should be more accurate, it is more computationally expensive.

## 5 Bounding the error of the out-of-sample extension

In this section, we prove that the error of the out-of-sample extension is bounded in both cases of distance-based weights (Eq. 4.3) and the tangential-based weights (Eq. 4.5). It means that for any function  $\psi : \mathcal{M} \rightarrow \mathcal{N}$ , which agrees on a given set of data points and satisfies certain conditions, the out-of-sample extension  $\hat{\psi}(x)$  of the data point  $x$  is close to  $\psi(x)$ .

First, we prove the consistency of the algorithm. In other words, the out-of-sample extension of data points, which coverage to an already known data point, will converge to its already known image.

**Lemma 5.1.** *Assume  $x \in \mathcal{M}$ . If  $x \rightarrow x_j \in M$  then  $\hat{\psi}(x) \rightarrow \psi(x_j)$ .*

An intuition for the proof of Lemma 5.1 is that the distance from the point  $x_i \in M$  is inversely proportional to the weight of the equation  $y = \psi(x_i)$  in Eq. 2.6, therefore, when  $x \rightarrow x_i$ , the distance tends to 0 and the weight tends to  $\infty$ . Notice that when  $x = x_i$  then, according to Eq. 4.2,  $\lambda = \infty$  and the out-of-sample extension is undefined.

**Definition 5.2.** *The dataset  $M \subset \mathcal{M}$  is called a  $\delta$ -net of the manifold  $\mathcal{M}$  if for any data point  $x \in \mathcal{M}$  there is  $\tilde{x} \in M$  such that  $\|x - \tilde{x}\| \leq \delta$ .*

**Theorem 5.1.** *Assume that  $M$  is a  $\delta$ -net of  $\mathcal{M}$ . Let  $\psi : \mathcal{M} \rightarrow \mathcal{N}$  be a Lipschitz function with a constant  $K$ . If  $\varepsilon_1 = \delta$  and  $\hat{\psi}(x)$  is computed using the weights in Eq. 4.3, then  $\|\hat{\psi}(x) - \psi(x)\| \leq 3K\delta$ .*

*Proof.* We denote by  $N_\delta(x) = \{x_1, \dots, x_k\}$  the set of data points in the  $\varepsilon_1 = \delta$  neighborhood of  $x$ . It is easy to see that all the data points of  $\psi(x_i)$  are inside a ball  $B \subset \mathcal{N}$  of radius  $K\varepsilon_1$ . Therefore, the out-of-sample extension  $y$  is also in this ball, namely

$$\left\| \hat{\psi}(x) - \psi(x_i) \right\| < 2K\varepsilon_1. \quad (5.1)$$

Since  $\psi$  is a Lipschitz function and  $\|x - x_i\| < \varepsilon_1$ , we have

$$\|\psi(x_i) - \psi(x)\| < K\varepsilon_1. \quad (5.2)$$

By combining Eqs. (5.1) and (5.2), we get  $\left\| \hat{\psi}(x) - \psi(x) \right\| \leq \left\| \hat{\psi}(x) - \psi(x_i) \right\| + \|\psi(x_i) - \psi(x)\| \leq 3K\varepsilon_1$ .

□

Next, we show an identical result for the case where the weights from Eq. 4.5 are utilized to construct the covariance matrix  $W$ . Moreover, the approximations of the tangential spaces converge to the correct tangential space as  $\varepsilon_1$  tends to 0.

**Theorem 5.3.** *Let  $M$  be a  $\delta$ -net of  $\mathcal{M}$  and let  $\psi : \mathcal{M} \rightarrow \mathcal{N}$  be a Lipschitz function with a constant  $K$ . If  $\varepsilon_1 = \delta$  and  $\hat{\psi}(x)$  is computed using the weights in Eq. 4.5, then  $\|\hat{\psi}(x) - \psi(x)\| \leq 3K\delta$ .*

*Proof.* Let  $N_\delta(x) = \{x_1, \dots, x_k\}$  be the  $\delta$  neighborhood of  $x$ . Then, the weight matrix becomes

$$W = \begin{pmatrix} w_1 & 0 & \dots & 0 \\ 0 & w_2 & \dots & 0 \\ & \vdots & \ddots & \\ 0 & \dots & 0 & w_k \end{pmatrix}.$$

By using Eq. (2.8), we get

$$\hat{\psi}(x) = \left( \sum w_i \right)^{-1} \sum w_i \psi(x_i), \quad (5.3)$$

where the  $w_i$  matrices are defined in Eq. 4.5. The structure of the  $w_i$  matrices allows us to find a basis in which all the matrices  $w_i$  become diagonal. Let us denote the diagonal form of  $w_i$  by  $D_i$ . Then  $D_i = Tw_iT^{-1}$  where  $T$  is the transformation matrix. We can rewrite Eq. (5.3) to become

$$\begin{aligned} T\hat{\psi}(y) &= T \left( \sum w_i \right)^{-1} T^{-1} T \sum w_i \psi(x_i) \\ &= \left( \sum Tw_iT^{-1} \right)^{-1} \sum Tw_iT^{-1} T \psi(x_i) \\ &= \left( \sum D_i \right)^{-1} \sum D_i T \psi(x_i). \end{aligned}$$

Since all  $D_i$  are diagonal, we get a weighted average of the data points  $\psi(x_i)$  in the new basis, which is known to be in convex hull. Thus, it is located inside a ball that contains all the data points. It means that  $\hat{\psi}(x)$  is inside a ball of radius  $K\varepsilon_1$  that contains all  $\psi(x_i)$ . Therefore,

$$\begin{aligned} \|\hat{\psi}(x) - \psi(x)\| &= \|\hat{\psi}(x) - \psi(x_i) + \psi(x_i) - \psi(x)\| \\ &\leq \|\hat{\psi}(x) - \psi(x_i)\| + \|\psi(x_i) - \psi(x)\| \\ &\leq 2K\varepsilon_1 + K\varepsilon_1 = 3K\varepsilon_1 = 3K\delta. \end{aligned}$$

□

## 6 Out-of-sample extension complexity

Recall that the dataset  $M$  consists of  $p$  data points and assume that the number of data points in the neighborhood of  $x$  is  $k$ . The covariance matrix of a data point  $\psi(x_j)$  from Eq. 4.4 is also computed once for each data point in  $M$ , considering each of its  $k$  neighbors. The complexity of the neighborhood computation is  $O(p)$  operations. Then, the covariance matrix is computed in  $O(dk^2)$  operations. Thus, the complexity of this

pre-computation stage is  $O(p \cdot (p + dk^2)) = O(p^2)$  operations. For each data point, we multiply vectors of size  $d \cdot k$  by matrices of size  $k \times d \cdot k$  or  $k \times k$ . Thus, the out-of-sample extension complexity is  $O(k^2 \times d^2)$  operations.

## 7 Experimental results

### 7.1 Example I: Data points on a sphere

The function  $\psi : [0, \pi] \times [0, \pi] \rightarrow \mathbb{R}^3$  maps the spherical coordinates  $(\phi, \theta)$  into a 3-D sphere of radius 1. More specifically,  $\psi(\phi, \theta) = (\sin(\phi) \cos(\theta), \sin(\phi) \sin(\theta), \cos(\phi))$ . We generate 900 data points angularly equally distributed where we have 30 data points on each axis as a training dataset. We generate 100 random data points for which we compute the out-of-sample extension. The results from the application of the algorithm using weights as defined in Eq. 4.3, are shown in Fig. 7.1. In Fig. 7.2, we can see three different results from an out-of-sample extension using different weights as presented in Section 4. In Table 7.1, we show how the results get better for more advanced weight algorithms. We display an accurate error mean for the algorithm. We also show the improvement of the results when we take 2500 data points angularly equally distributed with 50 data points on each axis:

Algorithm type	Color in Fig. 7.2	Mean error for 900 data points	Mean error for 2500 data points
Weights as in Eq. 4.3	Yellow	$1.04 \cdot 10^{-2}$	$6.01 \cdot 10^{-3}$
Weights as in Eq. 4.5	Red	$8.08 \cdot 10^{-3}$	$4.45 \cdot 10^{-3}$
Weights as in Eq. 4.5 but with different estimations for the tangential space at each data point	Black	$6.14 \cdot 10^{-3}$	$3.17 \cdot 10^{-3}$

Table 7.1: The mean error performances of the algorithms for different number of data points and different weights

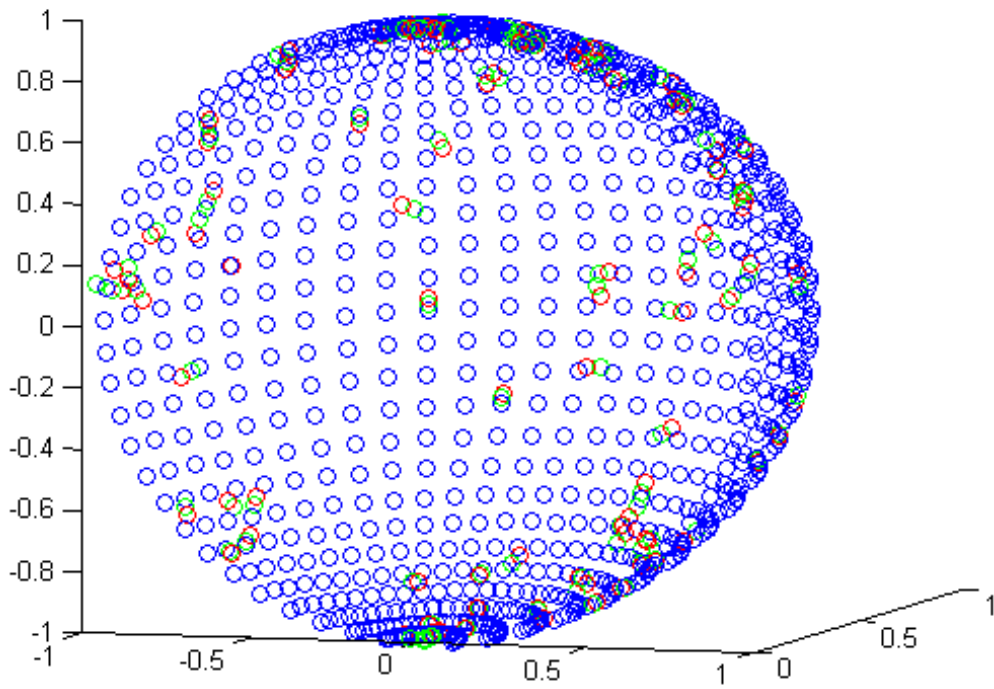


Figure 7.1: An illustration of the out-of-sample extension algorithm on a sphere. Blue - the original data set, green - the correct images, red - the out-of-sample extension calculated using the algorithm with weights from Eq. 4.3.

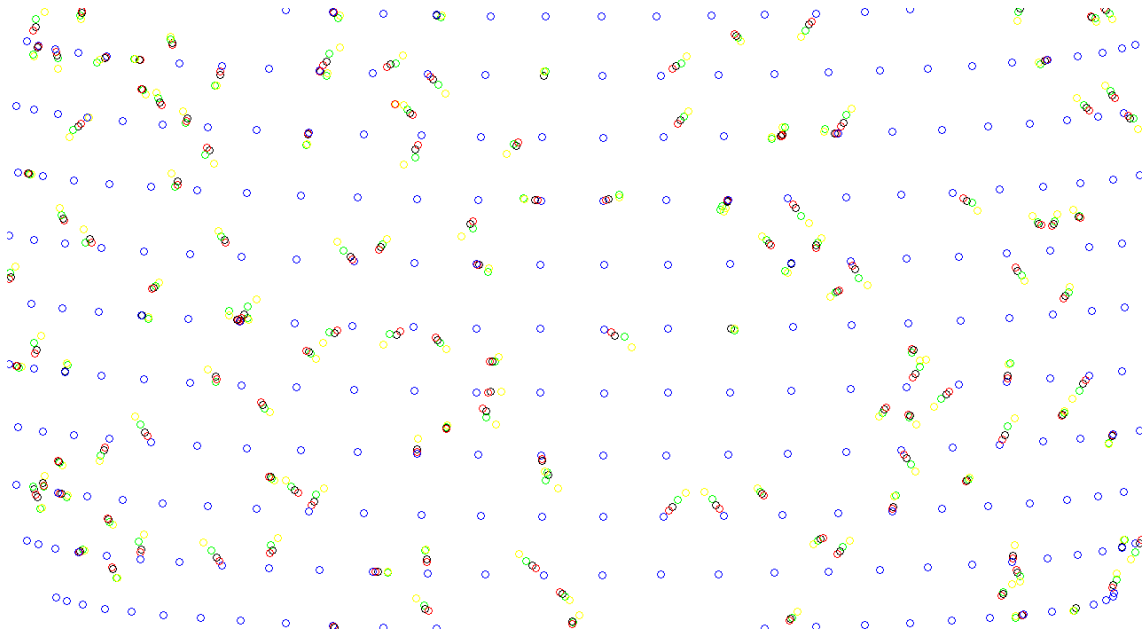


Figure 7.2: An illustration of the algorithms on a sphere in Table 7.1. Blue - the original data set, green - the correct images. yellow - the out-of-sample extension computed using the algorithm with weights from Eq. 4.3. Red - the out-of-sample extension computed using the algorithm with weights from Eq. 4.5. Black - the out-of-sample extension computed using the weights from Eq. 4.5, but with different estimations for the tangential space at each data point.

## 7.2 Example II: Dimensionality reduction example

DARPA datasets [16] from 1998 and 1999 are utilized here to find anomalies in them. All the activities and non-activities are labeled and published. These datasets contain different types of cyber attacks that we consider as anomalies.

We use this dataset to evaluate the performance of the out-of-sample extension using weights from Eq. 4.5 and the Mahalanobis distance from Eq. 2.9. The experiment done by following the example in [8]. We use the same data and same mapping that was developed in [8]. Diffusion Maps (DM) [6], which was applied to DARPA data, reduces the dimensionality by embedding  $\mathbb{R}^{14}$  to  $\mathbb{R}^5$  such that  $\psi : \mathbb{R}^{14} \rightarrow \mathbb{R}^5$ .

We present two experiments using this data to evaluate the performance of the out-of-sample extension. The first experiment is an out-of-sample extension for non-anomalous data points by comparing the original results from the DM embedding. The second experiment evaluates the anomaly detection of the algorithm.

### 7.2.1 Out-of-sample extension on DARPA data

In this experiment, we use 800 data points and an embedding function  $\psi : \mathbb{R}^{14} \rightarrow \mathbb{R}^5$  that was described before. By taking a random subset  $\{x_1, \dots, x_k\}$  of data points and by using the values  $\{\psi(x_1), \dots, \psi(x_k)\}$ , we approximate  $\psi$  on 50 data from the 800. We compare the approximated result to the correct values of  $\psi$  and measure the error. To evaluate the performance of our method, we compare these results to the results from other leading methods such as the classic Nyström method, the Multiscale data sampling and function extension (MSE) method described in [3,4] and the auto-adaptative Laplacian Pyramids method described in [18].

To make the presentation self contained, Nyström, MSE and auto-adaptative Laplacian pyramids methods are outlined next.

**Nyström method:** The Nyström method [1, 17] is vastly used for an out-of-sample extension in dimensionality reduction methods. It is a numerical scheme for the extension of integral operator eigenfunctions. It finds a numerical approximation for the eigenfunction problem

$$\int_a^b G(x, y)\phi(y)dy = \lambda\phi(x) \quad (7.1)$$

where  $\phi$  is an eigenfunction and  $\lambda$  is the corresponding eigenvalue. Given a set of equidistant points  $\{x_j\}_{j=1}^n \subset [a, b]$ . Assume that  $G$  is similarity matrix that is defined on the data whose  $(i, j)$  entry measures the similarity between the data points  $x_i$  and  $x_j$ , namely

$$G \triangleq \begin{bmatrix} g(x_1, x_1) & g(x_1, x_2) & \cdots & g(x_1, x_n) \\ g(x_2, x_1) & g(x_2, x_2) & \cdots & g(x_2, x_n) \\ \vdots & \vdots & \ddots & \vdots \\ g(x_n, x_1) & g(x_n, x_2) & \cdots & g(x_n, x_n) \end{bmatrix}. \quad (7.2)$$

A Gaussian function is a popular choice for  $g$ , and it is given by

$$g_\epsilon(x, x') \triangleq \exp\left(-\|x - x'\|^2 / \epsilon\right), \quad (7.3)$$

where  $\|\cdot\|$  constitutes a metric on the space. Then, Eq. 7.1 can be approximated by a quadrature rule to become  $\frac{b-a}{n} \sum_{j=1}^n G(x_i, x_j)\phi(x_j) = \lambda\phi(x_i)$ . Then, the Nyström extension of  $\phi$  to a new data point  $x_*$  is  $\hat{\phi}(x_*) \triangleq \frac{b-a}{n\lambda} \sum_{j=1}^n G(x_*, x_j)\phi(x_j)$ .



If  $G$  is symmetric, then its normalized eigenfunctions  $\{\phi_i\}_{i=1}^n$  constitute an orthonormal basis to  $\mathbb{R}^n$ . Thus, any vector  $f = [f_1 \ f_2 \ \dots \ f_n]^T$ , ( $f_j = f(x_j)$ ,  $j = 1, \dots, n$ ) can be decomposed into a superposition of its eigenvectors  $f = \sum_{i=1}^n (f^T \cdot \phi_i) \phi_i$ . Then, the Nyström extension of  $f$  to  $x_*$  becomes  $f_* \triangleq \sum_{i=1}^n (f^T \cdot \phi_i) \hat{\phi}_i(x_*)$ .

### MSE method:

---

**Algorithm 7.1:** Randomized interpolative decomposition

**Input:** An  $m \times n$  matrix  $A$  and an integer  $l$ , s.t.  $l < \min\{m, n\}$ .

**Output:** An  $m \times l$  matrix  $B$  and an  $l \times n$  matrix  $P$  that satisfies  $\|A - BP\| \lesssim l\sqrt{mn}\sigma_{l+1}(A)$

---

- 1: Use a random number generator to form a real  $l \times n$  matrix  $G$  whose entries are i.i.d Gaussian random variables of zero mean and unit variance. Compute the  $l \times n$  product matrix  $W = GA$ .
- 2: Apply the pivoted QR routine to  $W$  (Algorithm 5.4.1 in [11]),  $WP_R = QR$ , where  $P_R$  is an  $n \times n$  permutation matrix,  $Q$  is an  $l \times l$  orthogonal matrix, and  $R$  is an  $l \times n$  upper triangular matrix, where the absolute values of the diagonal are ordered decreasingly.
- 3: Split  $R$  s.t.

$$R = \left( \begin{array}{c|c} R_{11} & R_{12} \\ \hline 0 & R_{22} \end{array} \right),$$

where  $R_{11}$  is  $l \times l$ ,  $R_{12}$  is  $l \times (n - l)$  and  $R_{22}$  is  $(n - l) \times (n - l)$ .

- 4: Define the  $l \times l$  matrix  $S = QR_{11}$ .
  - 5: From Step 4, the columns of  $S$  constitute a subset of the columns of  $W$ . In other words, there exists a finite sequence  $i_1, i_2, \dots, i_{l-1}, i_l$  of integers such that, for any  $j = 1, 2, \dots, l - 1, l$ , the  $j$ th column of  $S$  is the  $i_j$ th column of  $W$ . The corresponding columns of  $A$  are collected into a real  $n \times l$  matrix  $B$ , so that, for any  $j = 1, 2, \dots, l - 1, l$ , the  $j$ th column of  $B$  is the  $i_j$ th column of  $A$ . Then, the sampled dataset is  $D_s = \{x_{i_1}, x_{i_2}, \dots, x_{i_{l-1}}, x_{i_l}\}$ .
-

---

**Algorithm 7.2:** Single-scale extension

---

**Input:**  $N \times l_s$  matrix  $B_s$ , the associated sampled data  $D_s = \{x_{i_1}, x_{i_2}, \dots, x_{i_{l_s}}, x_{i_l}\}$ , a new data point  $x$  and a function  $\bar{f} = (f(x_1) f(x_2) \dots f(x_n))^T$  to be extended.

**Output:** The projection  $\bar{f}_s = (f_s(x_1), f_s(x_2), \dots, f_s(x_n))^T$  of  $f$  on the numerical range of the associated kernel matrix, its extension  $f_s(x)$  to  $x$ , and the sampled dataset  $D_s$ .

---

- 1: Apply SVD to  $B_s$ , s.t.  $B_s = U_s \Sigma_s V_s^*$ .
- 2: Calculate the pseudo-inverse  $B_s^\dagger = V_s \Sigma_s^{-1} U_s^*$  of  $B_s$ .
- 3: Calculate the coordinates vector  $c = (c_1, c_2, \dots, c_{l_s})^T = B_s^\dagger \bar{f}$  of the orthogonal projection of  $\bar{f}_s$  on the range of  $B_s$  in the basis of  $B_s$ 's columns.
- 4: Calculate the orthogonal projection  $\bar{f}_s = B_s c$  of  $f$  on  $B_s$ .
- 5: Calculate the extension of  $\bar{f}_s$  to  $x$  s.t.

$$f_s(x) = (g_s(\|x - x_{s_1}\|), g_s(\|x - x_{s_2}\|), \dots, g_s(\|x - x_{s_{l_s}}\|)) c.$$

---

---

**Algorithm 7.3:** MSE

---

**Input:** A dataset  $D = \{x_1, \dots, x_n\}$  in  $\mathbb{R}^d$ , a positive number  $T > 0$ , a new data point  $x \in \mathbb{R}^d \setminus D$ , a function  $\bar{f} = (f(x_1) f(x_2) \dots f(x_n))^T$  to be extended and an error parameter  $err \geq 0$ .

**Output:** An approximation  $\bar{G} = (G(x_1), G(x_2), \dots, G(x_n))^T$  of  $f$  on  $D$  and its extension  $G(x)$  to  $x$ .

---

- 1: Set the scale parameter  $s = 0$ ,  $\bar{F}_{-1} = 0$  and  $F_{-1}(x) = 0$ .
  - 2: **while**  $\|\bar{f} - \bar{F}_{s-1}\| > err$  **do**
  - 3: Form the Gaussian kernel  $K_s$  on  $D$  (see  $(K_\epsilon)_{ij} = g_\epsilon(\|x_i - x_j\|)$ ,  $i, j = 1, \dots, N$ ), with  $\epsilon_s = \frac{T}{2^s}$ .
  - 4: Estimate the numerical rank  $l_s$  of  $K_s$  using  $R_\delta(K_\epsilon) \leq \prod_{i=1}^d C(|I_i|, \epsilon, \delta)$ .
  - 5: Apply Algorithm 7.1 to  $K_s$  and  $l_s$  to get an  $n \times l_s$  matrix  $B_s$  and sampled dataset  $D_s$ .
  - 6: Apply Algorithm 7.2 to  $B_s$  and  $\bar{f}$ . We get the approximation  $\bar{f}_s$  to  $\bar{f} - \bar{F}_{s-1}$  at scale  $s$ , and its extension  $f_s(x)$  to  $x$ .
  - 7: Set  $\bar{F}_s = \bar{F}_{s-1} + \bar{f}_s$ ,  $F_s(x) = F_{s-1}(x) + f_s(x)$ ,  $s = s + 1$ .
  - 8: **end while**
  - 9:  $\bar{G} = \bar{F}_{s-1}$  and  $G(x) = F_{s-1}(x)$ .
- 

**Laplacian Pyramid method:** The Laplacian pyramid is a multi-scale algorithm for

extending an empirical function  $f$ , which is defined on a dataset  $\Gamma$ , to new data points. Mutual distances between the data points in  $\Gamma$  are used to approximate  $f$  in different resolutions.

$\Gamma$  is a set of  $n$  data points in  $\mathbb{R}^m$  and  $f$  is a function defined on  $\Gamma$ . A Gaussian kernel is defined on  $\Gamma$  as  $W_0 \triangleq w_0(x_i, x_j) = e^{\frac{-\|x_i - x_j\|^2}{\sigma_0}}$ . Normalizing  $W_0$  by  $K_0 = k_0(x_i, x_j) = q_0^{-1}(x_i)w_0(x_i, x_j)$  where  $q_0(x_i) = \sum_j w_0(x_i, x_j)$ , yields a smoothing operator  $K_0$ . At a finer scale  $l$ , the Gaussian kernel  $W_l = w_l(x_i, x_j) = e^{-\|(x_i - x_j)\|^2 / (\frac{\sigma_0}{2^l})}$  yields the smoothing operator  $K_l = k_l(x_i, x_j) = q_l^{-1}(x_i)w_l(x_i, x_j)$ .

For any function  $f : \Gamma \rightarrow \mathbb{R}$ , the Laplacian Pyramid representation of  $f$  is defined iteratively as follows:

$$\begin{aligned} s_0(x_k) &= \sum_{i=1}^n k_0(x_i, x_k) f(x_i) && \text{for level } l = 0 \\ s_l(x_k) &= \sum_{i=1}^n k_l(x_i, x_k) d_l(x_i) && \text{otherwise.} \end{aligned} \tag{7.4}$$

The differences

$$\begin{aligned} d_1 &= f - s_0 && \text{for level } l = 1 \\ d_l &= f - \sum_{i=0}^{l-1} s_i && \text{for level } l \geq 1 \end{aligned} \tag{7.5}$$

are input for this algorithm at level  $l$ .

Equation (7.4) approximates a given function  $f$  in a multi-scale manner, where  $f \approx s_0 + s_1 + s_2 + \dots$ . An admissible error should be set a-priori and the iterations in Eq. (7.4) stop when  $\|f - \sum_k s_k\| < \text{err}$ .

We extend  $f$  to a new point  $y \in \mathbb{R}^m \setminus \Gamma$  in the following way:

$$\begin{aligned} s_0(y) &= \sum_{i=1}^n k_0(x_i, y) f(x_i) && \text{for level } l = 0 \\ s_l(y) &= \sum_{i=1}^n k_l(x_i, y) d_l(x_i) && \text{otherwise.} \end{aligned} \tag{7.6}$$

The extension of  $f$  to the point  $y$  is evaluated from Eq. (7.6) as  $f(y) = \sum_k s_k(y)$ .

The performance results of the 4 methods are shown in Fig.7.3.

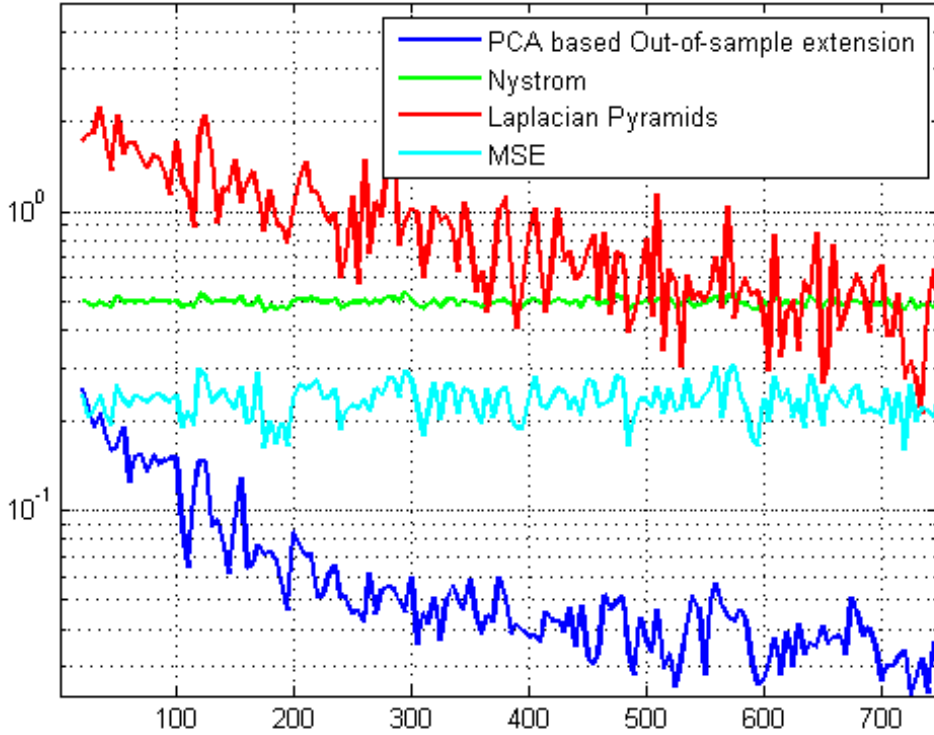


Figure 7.3: Performance comparison between different out-of-sample extension methods. The x-axis is the size of the training set and the y-axis is the norm of the error from the out-of-sample extension methods.

### 7.2.2 Anomaly detection on DARPA data

In this experiment, all the 1321 available data points are used as our training dataset. We show in Fig. 7.4 the image of these data points after the embedding by  $\psi$ . The normal behaved manifold in the embedded space in Fig. 7.4 has the “horseshoe” shape. We can see a few data points, which are classified as anomalous, are the labeled attacks. Then, a set of newly arrived data points are assigned with coordinates in the embedded space via the application of Nyström extension as can be seen in the left image in Fig. 7.5. It is also done by the application of the MSE algorithm in [4]. Data point #51, which is a newly arrived data point, is an anomalous that can be seen as an outlier on the left side of the normal (“horseshoe”) manifold.

We apply our out-of-sample extension algorithm using weights from Eq. 4.5, to the same set of newly arrived data points. The results are shown on the right image in Fig.

7.5. To find anomalies, we compute the Mahalanobis distance of the extension using Eq. (2.9) for each of the newly arrived data points. We see that data point #51 emerged as having a much higher residual error ( $2.7210^{-7}$ ) than the other data points whose average residual error is  $6.2110^{-10}$ . All the Mahalanobis distance values are shown in Fig. 7.6.

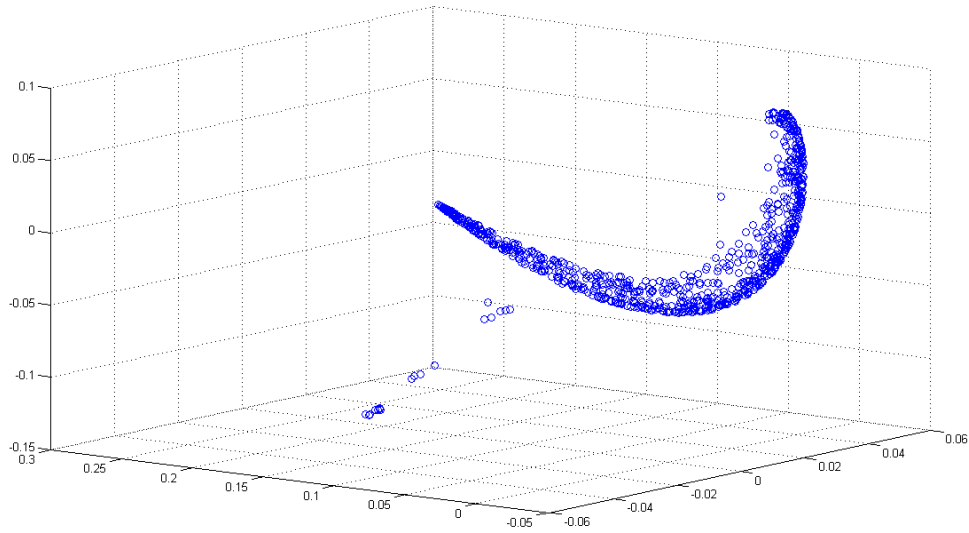


Figure 7.4: The first three coordinates of the data points in  $\mathbb{R}^{14}$  after its embedding into  $\mathbb{R}^5$ .

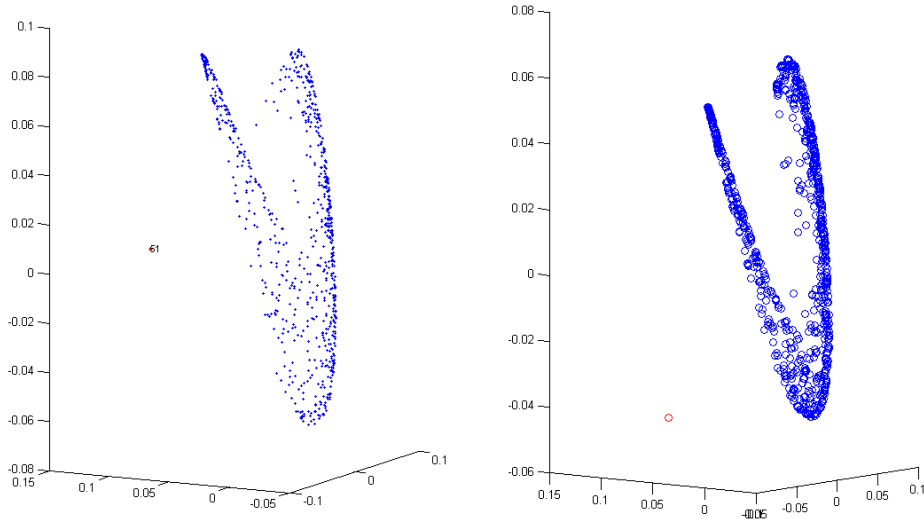


Figure 7.5: Out-of-sample extension computed for a new day. In the left side, the out-of-sample extension is computed via the application of the Nyström extension algorithm. Data point #51 is known to be an anomalous data point. In the right image, the output of the algorithm, which uses weights from Eq. 4.5, is presented by the red data point which is the data point # 51.

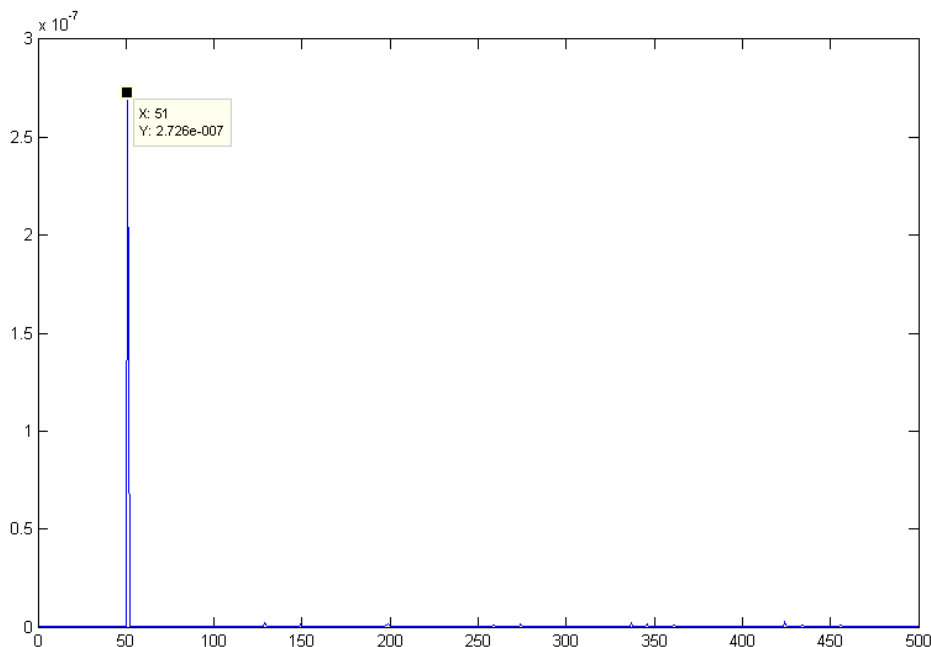


Figure 7.6: The Mahalanobis distance values. We see that data point #51 has the highest value. Therefore, it is classified as an anomalous data point.

## Conclusions

In this paper, we present an efficient out-of-sample extension (interpolation) scheme for dimensionality reduction maps that are widely used in the field of data analysis. The computational cost of such maps is high. Therefore, once such a map is computed over a training set, an efficient extension scheme is needed. The presented scheme is based on the manifold assumption, which is widely used in the field of dimensionality reduction. It provides an optimal solution from a stochastic geometric-based linear equations system that is determined by the application of local PCA of the embedded data. Moreover, the scheme enables to detect abnormal data points. The interpolation error was analyzed by assuming that the original map is a Lipschitz function. The scheme was applied to both synthetic and real-life data to provide good results by mapping data from the manifold to the image manifold and by detection of abnormal data points.

# Acknowledgments

This research was partially supported by the Israeli Ministry of Science & Technology (Grants No. 3-9096, 3-10898), US-Israel Binational Science Foundation (BSF 2012282), Blavatnik Computer Science Research Fund and ICRC Funds.

# References

- [1] C.T.H. Baker. *The Numerical Treatment of Integral Equations*. Oxford: Clarendon Press, 1977.
- [2] M. Belkin and P. Niyogi. Laplacian eigenmaps for dimensionality reduction and data representation. *Neural Computation*, 15:1373–1396, 2003.
- [3] A. Bermanis, A. Averbuch, and R.R. Coifman. Multiscale data sampling and function extension. *SampTA 2011*, 2011.
- [4] A. Bermanis, A. Averbuch, and R.R. Coifman. Multiscale data sampling and function extension. *Applied and Computational Harmonic Analysis*, 34:15–29, 2013.
- [5] M. D. Buhmann. Radial basis functions: Theory and implementations. Cambridge University Press, 2003.
- [6] R.R. Coifman and S. Lafon. Diffusion maps. *Applied and Computational Harmonic Analysis*, 21(1):5–30, 2006.
- [7] R.R. Coifman and S. Lafon. Geometric harmonics: A novel tool for multiscale out-of-sample extension of empirical functions. *Applied and Computational Harmonic Analysis*, 21(1):31–52, 2006.
- [8] G. David. *Anomaly Detection and Classification via Diffusion Processes in Hyper-Networks*. PhD thesis, School of Computer Science, Tel Aviv University, March 2009.
- [9] L.M Delves and J. Walsh. Numerical solution of integral equations. Clarendon, Oxford, 1974.



- [10] D.L. Donoho and C. Grimes. Hessian eigenmaps: New locally linear embedding techniques for high dimensional data. *Proceedings of the National Academy of Sciences of the United States of America*, 100:5591–5596, May 2003.
- [11] G. H. Golub and C. F. Van Loan. Matrix computations. The Johns Hopkins University Press, 3rd edition, 1996.
- [12] H. Hotelling. Analysis of a complex of statistical variables into principal components. *Journal of Educational Psychology*, 24, 1933.
- [13] I.T. Jolliffe. *Principal Component Analysis*. Springer, New York, NY, 1986.
- [14] T. Kariya and H. Kurata. *Generalized least squares*. Wiley, 2004.
- [15] A.V. Little, J. Lee, Yoon-Mo Jung, and M. Maggioni. Estimation of intrinsic dimensionality of samples from noisy low-dimensional manifolds in high dimensions with multiscale svd. In *Statistical Signal Processing, 2009. SSP '09. IEEE/SP 15th Workshop on*, pages 85 –88, 31 2009-sept. 3 2009.
- [16] Lincoln Laboratory MIT. Darpa intrusion detection evaluation data sets. [http://www.ll.mit.edu/IST/ideval/data/data\\_index.html](http://www.ll.mit.edu/IST/ideval/data/data_index.html), 1999.
- [17] W.H. Press, S.A. Teukolsky, W.T. Vetterling, and B.P. Flannery. *Numerical Recipes in C*. Cambridge Univ. Press, 2nd edition, 1992.
- [18] N. Rabin and R. R. Coifman. Heterogeneous datasets representation and learning using diffusion maps and laplacian pyramids. In *SDM*, pages 189–199, 2012.
- [19] N. Rabin and R.R. Coifman. Heterogeneous datasets representation and learning using diffusion maps and laplacian pyramids. *Proceedings of the 12th SIAM International Conference on Data Mining, SDM12.*, 2012.
- [20] S.T. Roweis and L.K. Saul. Nonlinear dimensionality reduction by locally linear embedding. *SCIENCE*, 290:2323–2326, 2000.
- [21] J. Schuetter and T. Shi. Multi-sample data spectroscopic clustering of large datasets using Nyström extension. *Journal of Computational and Graphical Statistics*, pages 531–542, 2011.

- [22] H. Wendland. Scattered data approximation. Cambridge University Press, 2005.
- [23] G. Yang, X. Xu, and J. Zhang. Manifold alignment via local tangent space alignment. *International Conference on Computer Science and Software Engineering*, December 2008.
- [24] Z. Zhang and H. Zha. Principal manifolds and nonlinear dimension reduction via local tangent space alignment. *SIAM Journal on Scientific Computing*, pages 313–338, 2004.